The Heat Capacity and Magnetization of Praseodymium Metal in the Temperature Region 1.2–4.2°K with Applied Magnetic Fields up to 40,000 G†

R. L. STEIN AND R. A. BUTERA

Department of Chemistry, University of Pittsburgh, Pittsburgh, Pennsylvania 15213

The magnetic and thermal properties of two spherical samples of Praseodymium have been determined over the temperature region 1.2–4.2°K in magnetic fields to 40 kG. The zero applied magnetic field heat capacity data indicate the existence of an anomaly centered about 3.4°K and an upturn below 1.4°K. The temperature of the small 3.4°K anomaly decreases as the field is increased. The temperature of the onset of the upturn, as well as its magnitude, increases as the magnetic field is applied. This behavior was exhibited by both samples; however, the absolute magnitude of the heat capacity differed between samples. The magnetization exhibited no unusual behavior at 3.4°K; however, the magnetic moment in a 5000 G applied field increased as the temperature decreased. A remnant moment was detected in one of the samples after the application of a magnetic field. The effect of impurities on the anomaly is discussed.

A considerable amount of interest has in recent years been directed towards the determination of the magnetic and thermal properties of the rare-earth metals. Of these results the most difficult to understand are those reported for praseodymium. Parkinson, Simon, and Spedding (*1*) determined the heat capacity of praseodymium over the temperature region 2.5–170°K. They reported a large Shottky-like anomaly centered at approximately 100°K. The excess entropy associated with this anomaly was 4.06 cal/mole°K. This compared favorably with the theoretical value of $R\ln 9$ (4.39 cal/mole°K) indicating that the crystal field entirely removed the degeneracy of the magnetic levels. Bleaney (*2, 3*) derived a splitting pattern with the associated hyperfine interaction for praseodymium which reasonably fit the specific heat and ESR data. He gives the crystal field ground state of the cubic sites as a singlet, with the next higher state split into a triplet, while the energy levels of the hexagonal sites are split into two low lying singlet states. Lock (*4*) and Graf (*5*) have reported that the magnetic susceptibility of Pr obeys the Curie–Weiss Law down to 100°K (with a paramagnetic Curie temperature of about 8°K). Below 100°K the susceptibility deviates from the Curie–Weiss Law and becomes temperature independent at 4°K, indicating

that Pr can be classified as a Van Vleck paramagnet. Cable et al. (*6*) have determined by neutron diffraction, that Pr becomes an antiferromagnet with a Neel temperature of approximately 25°K having a spin structure similar to that of neodymium.

The specific heat data of Parkinson et al. (*7*) give no evidence of a Neel point near 25°K. Data reported by Wallace and Craig (*8*), as well as by Lounasmaa and Sundstrom (*9*), confirm these findings.

Kissell (*10*) has determined that the low-temperature susceptibility of Pr is both field and sample dependent. At 4°K the susceptibility was found to decrease as the applied field was increased above 10 kG. The values of the magnetization found for various samples differed by as much as 10%. Also the magnetization along three mutually perpendicular axis of the same solid sample was found to differ by 5–10%. Wallace et al. (*11*) have recently developed an approach where "spontaneous induced magnetization" is used to successfully envelope the apparent contradiction in the previous data. The authors accurately predict the onset of ordering at 25°K and explain the drop in susceptibility at 4°K.

It is evident that the magnetic properties of praseodymium are not as yet well understood in the region above 4°K. The region below 4.2°K is, however, more complex.

Specific heat data reported by Dreyfus et al. (*12*)

and Dempsey, Gordon, and Soller (13) show what appears to be a large hyperfine interaction below 1°K with no unusual behavior occurring between 1 and 4°K. In addition, the magnitude of the experimental values of the heat capacity of Dreyfus et al. (12) and Dempsey et al. (13) differ from each other by as much as 10%. Lounasmaa (14) conducted extensive heat capacity measurements on Pr in this region and reported some rather unusual behavior. In addition to obtaining different values of the specific heat than either Dreyfus et al. (12) or Dempsey et al (13) the heat capacity exhibited a kink centered about 3.4°K. Dixon (15) has also reported the existence of the kink in the heat capacity at 3.4°K but his results again differed in magnitude.

We have directed our efforts toward resolving the nature of both the low-temperature upturn and the 3.4°K kink in the specific heat. The extensive study was undertaken for several reasons:

(1) To determine why all Pr samples studied give varying results for the specific heat in the liquid helium region;

(2) To determine if the 3.4°K anomaly exists, and how it would react under the influence of a magnetic field;

(3) To determine if the magnetization is truly temperature independent below 4°K;

(4) To clarify the hyperfine interaction near 1°K.

Sample Preparation

The praseodymium samples used in this study (designated Pr II and Pr III) were both prepared in a similar fashion. The samples obtained from the supplier were machined under oil into 1.250-in. diameter spheres. Upon final polishing and cleaning, the sample was weighed and then coated with a layer of Dow vacuum silicon grease as well as high conductivity copper impregnated grease. It was then placed into the apparatus and the space around the sample immediately evacuated, thereby keeping the oxides which may have formed on the sphere surface to a minimum. The weight of vacuum and high conductivity grease was negligible and their heat capacity could thus be ignored.

He^4 exchange gas was used to cool the samples to 4.2°K where it was liquified via conduction from an upper one liter He^4 coolant container. The liquid in the cooling chamber was pumped so that the sample was brought to temperatures below 1.2°K. The sample was than isolated by further pumping on the cooling chamber line to remove the liquid He^4

and produce a vacuum of at least 1×10^{-5} mm Hg. The main insulating vacuum was better than 10^{-6} mm Hg and was continually monitored by a mass-spectrometer type leak detector. The upper one liter He^4 pot was pumped and maintained below 2°K to minimize heat leak to the sample.

Upon completion of preliminary magnetization measurements, the Pr II same was submitted for analysis. While the supplier (16) included an analysis of the sample, which showed no impurities greater than 0.2%, the sample had a remnant moment which suggested that the supplier's analysis may have been in error.

Two separate methods of analysis were used. X-ray fluorescence spectroscopy (17) showed that the concentration of both Nd and Ce, the major contaminants, were less than 0.1%. Spectrochemical analysis (18) was also performed. Metal filings of Pr were used directly with graphite powder in a graphite electrode. The analysis using an Ebert Mounting Spectrograph showed that Nd and Ce were present in amounts of less than 0.2%. All other metals were present in amounts of less than 0.02% (Tb, Y) or smaller (Fe, 0.001%; Eu, 0.02%; Co, 0.001%). No other metals were detected.

Since the above results agreed closely with the original analysis for Pr II, the Pr III sample was not reanalyzed. The following is the analysis of the Pr III sample as reported by Research Chemicals:

Impurity	Percent
Ln	0.02
Yt	0.02
Ca	0.01
Mg	0.01
Si	0.03
Fe	0.01
Al	0.01
Cu	0.01

All other metals were undetected.

Experimental Results

Prior to the determination of the in-field heat capacity, a cursory set of magnetization measurements was obtained for each sample. These results are shown in Figs. 1, 2, and 3.

The M vs H curve at a temperature of 1.2°K is significant in two respects; one, that the two samples show no unusual behavior up to 30,000 G; and two, that the infinite field extrapolated saturation value
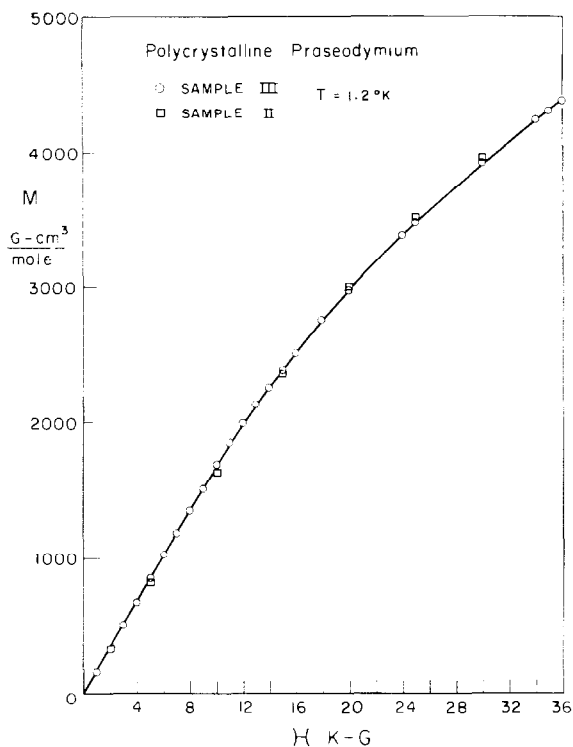
FIG. 1. Field variation of the magnetization for samples Pr II and Pr III at 1.2°K.

FIG. 3. $1/M$ vs T for samples Pr II and Pr III at 5000 G.

of the magnetization is equal to approximately one-half the praseodymium free-ion moment value of 3.2 Bohr magnetons.

FIG. 2. Temperature variation of the magnetization for samples Pr II and Pr III at 5000 G.

The M vs T curve at a constant applied field of 5000 G shows no unusual behavior at 3.4°K to indicate magnetic ordering. It is significant that both samples, while giving different absolute values of magnetization, given the identical qualitative indications of increasing moment with decreasing temperature.

The most striking difference between these two samples is the existence of a zero field moment on Sample Pr II after the application of a magnetic field. The magnitude of the remnant magnetization was found to be dependent only on the maximum value of the previously applied magnetic field up to approximately 20,000 G at which saturation occurred. This field dependency of the remnant moment is shown in Fig. 4. No zero-field moment was detected on sample Pr III at any time.

A plot of the zero-field heat capacity is given in Fig. 5. The experimental observations are tabulated in Table I. These results are compared with the earlier heat capacity data of Dixon (15) and Lounasmaa (19) for praseodymium. These data are plotted in terms of C_H/T vs T^2 so that the small anomaly centered about 3.4°K is more easily recognizable.

Figure 5 consists of several series of measurements covering this temperature region. These series agree quite well and were made in successive runs within a 36-hr period. Although the carbon resistance thermometer had a long history of reproduc-
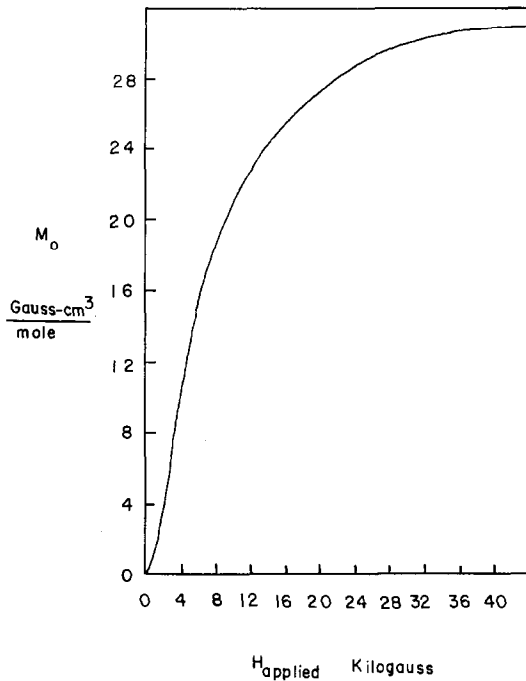
FIG. 4. Magnetic field dependency of the remnant moment of sample Pr II.
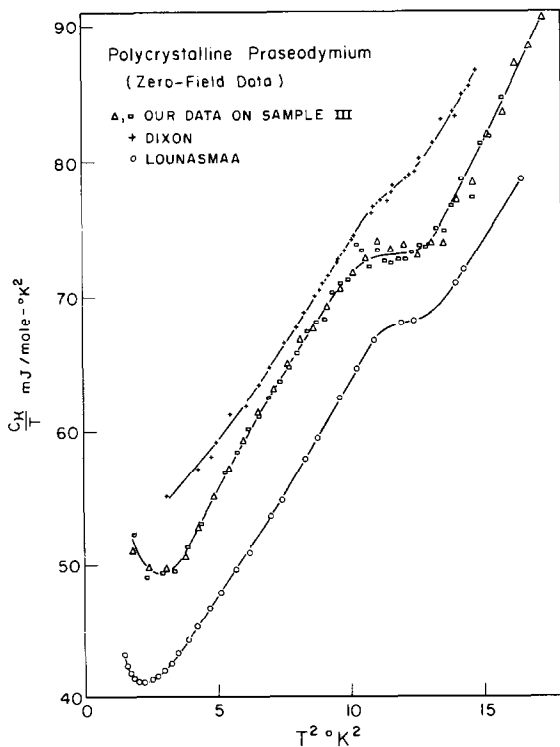
ibility upon temperature cycling, once a sample was brought to liquid He^4 temperatures, all measurements and calibrations were completed before the sample temperature was allowed to increase above liquid He^4 temperatures.

The question of the existence of the 3.4°K anomaly is now answered affirmatively. Earlier work on praseodymium failed to show any slope change in the heat capacity corresponding to this kink. The low-temperature upturn in the specific heat in our sample occurs approximately at the same temperature as that reported by Lounasmaa.

The in-field heat capacity for our first sample, designated Pr III, is shown in Figs. 6 and 7. The zero-field heat capacity is also plotted in Fig. 6 for comparison purposes in terms of C/T vs T for clarity in the features of interest. These experimental observations are tabulated in Table I. There are three major effects occurring as the field is increased to 30,000 G:

(1) The kink has begun to move down in temperature as the field is increased until at 30,000 G it occurs at approximately 2.6°K.

(2) The total heat capacity decreases for temperatures above the upturn. The total entropy

FIG. 5. Zero-Field heat capacity for sample Pr III.

FIG. 6. In-Field heat capacity for sample Pr III ($H = 0$–30 kG).

TABLE I

Experimental Heat Capacity Data for Polycrystalline Praseodymium Sample III

T(initial) °K	T(final) °K	C_H Joules / mole-°K	T(initial) °K	T(final) °K	C_H Joules / mole-°K
		H = 0 Series 1			**H = 0 Series 2**
1.1575	1.2273	0.079	1.2723	1.4178	0.071
1.2973	1.4040	0.071	1.4803	1.6178	0.077
1.4683	1.5704	0.075	1.6803	1.8043	0.086
1.6368	1.7303	0.083	1.8595	1.9723	0.096
1.7902	1.8770	0.090	2.0205	2.1221	0.109
1.9311	2.0101	0.101	2.1632	2.2554	0.121
2.0576	2.1302	0.111	2.2908	2.3754	0.133
2.1721	2.2391	0.121	2.4059	2.4967	0.145
2.2761	2.3385	0.131	2.5224	2.6065	0.157
2.3713	2.4300	0.140	2.6285	2.7073	0.168
2.4591	2.5144	0.149	2.7259	2.8000	0.179
2.5405	2.5933	0.157	2.8160	2.8859	0.190
2.6166	2.6670	0.165	2.9004	2.9773	0.199
2.6878	2.7359	0.173	2.9890	3.0618	0.210
2.7545	2.8008	0.180	3.0720	3.1415	0.220
2.8178	2.8623	0.187	3.1499	3.2167	0.229
2.8776	2.9202	0.196	3.2238	3.2882	0.238
2.9339	2.9754	0.202	3.2945	3.3564	0.247
2.9874	3.0281	0.206	3.3619	3.4310	0.251
3.0390	3.0778	0.216	3.4357	3.5031	0.257
3.0878	3.1256	0.221	3.5064	3.5730	0.259
3.1344	3.1719	0.222	3.5760	3.6405	0.267
3.1800	3.2153	0.237	3.6431	3.7064	0.272
3.2228	3.2577	0.239	3.7090	3.7845	0.289
3.2648	3.2998	0.238	3.7864	3.8593	0.299
3.3060	3.3400	0.245	3.8608	3.9295	0.318
3.3457	3.3795	0.246	3.9310	3.9974	0.330
3.3847	3.4184	0.247	3.9999	4.0626	0.349
3.4231	3.4564	0.251	4.0643	4.1253	0.359
3.4605	3.4933	0.254			
3.4971	3.5292	0.259			**H = 10,000 Series 1**
3.5325	3.5640	0.263			
3.5667	3.6111	0.264	1.1723	1.2226	0.108
3.6127	3.6559	0.272	1.2842	1.3694	0.073
3.6576	3.7003	0.275	1.4342	1.5321	0.077
3.7013	3.7489	0.285	1.5937	1.6866	0.082
3.7495	3.7960	0.297	1.7466	1.8511	0.089
3.7966	3.8422	0.295	1.9039	1.9992	0.100
3.8418	3.8846	0.314	2.0478	2.1353	0.110
3.8844	3.9386	0.320	2.1777	2.2588	0.120
3.9379	3.9898	0.334	2.2959	2.3713	0.131
3.9883	4.0391	0.341	2.4034	2.4740	0.140
4.0367	4.0868	0.345	2.5022	2.5684	0.150
4.0852	4.1315	0.375	2.5931	2.6645	0.160

Table I (cont.)

$T_{(initial)}$ °K	$T_{(final)}$ °K	C_H Joules/mole-°K	$T_{(initial)}$ °K	$T_{(final)}$ °K	C_H Joules/mole-°K
2.6860	2.7534	0.170	3.8459	3.9269	0.299
2.7718	2.8356	0.179	3.9170	3.9923	0.323
2.8518	2.9225	0.189	3.9867	4.0575	0.345
2.9365	3.0036	0.199	4.0516	4.1227	0.341
3.0152	3.0794	0.208	4.1160	4.1821	0.369
3.0894	3.1602	0.216			
3.1681	3.2458	0.224		H = 20KG Series 1	
3.2521	3.3275	0.231			
3.3320	3.4053	0.237	1.3125	1.4078	0.079
3.4086	3.4807	0.240	1.4729	1.5689	0.078
3.4819	3.5516	0.248	1.6387	1.7306	0.083
3.5523	3.6282	0.257	1.7985	1.8868	0.087
3.6279	3.7003	0.270	1.9506	2.0329	0.094
3.6985	3.7751	0.285	2.0911	2.1676	0.102
3.7728	3.8481	0.289	2.2209	2.2922	0.111
3.8446	3.9224	0.313	2.3432	2.4168	0.120
3.9188	3.9952	0.318	2.4659	2.5351	0.128
3.9972	4.0662	0.355	2.5824	2.6471	0.138
4.0636	4.1340	0.346	2.6926	2.7533	0.147
4.1330	4.1999	0.365	2.7976	2.8591	0.156
			2.9010	2.9595	0.164
	H = 10KG Series 2		3.0000	3.0560	0.172
			3.0952	3.1494	0.177
1.1814	1.2800	0.077	3.1874	3.2404	0.180
1.3430	1.4432	0.075	3.2765	3.3275	0.187
1.5012	1.5962	0.080	3.3610	3.4107	0.191
1.6510	1.7416	0.085	3.4409	3.4874	0.205
1.7948	1.8790	0.092	3.5160	3.5609	0.212
1.9272	2.0050	0.101	3.5842	3.6274	0.222
2.0496	2.1217	0.110	3.6489	3.6906	0.229
2.1624	2.2294	0.120	3.7105	3.7508	0.238
2.2652	2.3394	0.129	3.7699	3.8087	0.246
2.3709	2.4407	0.138	3.8266	3.8632	0.262
2.4676	2.5503	0.149	3.8798	3.9439	0.264
2.5734	2.6505	0.158	3.9555	4.0116	0.305
2.6703	2.7416	0.170	4.0303	4.0904	0.281
2.7581	2.8262	0.179	4.1010	4.1549	0.317
2.8404	2.9051	0.189			
2.9171	2.9787	0.198		H = 20KG Series 2	
2.9890	3.0543	0.206			
3.0624	3.1251	0.215	1.1578	1.2462	0.087
3.1318	3.2096	0.223	1.3125	1.4063	0.081
3.2141	3.2905	0.227	1.4702	1.5671	0.078
3.2939	3.3674	0.236	1.6329	1.7257	0.082
3.3696	3.4409	0.243	1.7863	1.8756	0.086
3.4414	3.5296	0.247	1.9315	2.0148	0.093
3.5281	3.6128	0.257	2.0649	2.1428	0.101
3.6102	3.6909	0.270	2.1871	2.2603	0.108
3.6871	3.7743	0.278	2.2995	2.3683	0.116
3.7690	3.8508	0.297	2.4027	2.4676	0.123

Table I (cont.)

T(initial) °K	T(final) °K	C_H Joules / mole-°K	T(initial) °K	T(final) °K	C_H Joules / mole-°K
2.4982	2.5709	0.132	3.5063	3.5842	0.188
2.5974	2.6665	0.139	3.5858	3.6598	0.199
2.6894	2.7546	0.147	3.6601	3.7314	0.206
2.7745	2.8375	0.153	3.7316	3.8082	0.218
2.8547	2.9150	0.159	3.8075	3.8814	0.227
2.9300	2.9876	0.167	3.8801	3.9695	0.237
3.0007	3.0568	0.171	3.9677	4.0511	0.255
3.0675	3.1318	0.175	4.0485	4.1274	0.270
3.1405	3.2029	0.180	4.1256	4.2179	0.285
3.2100	3.2712	0.183			
3.2770	3.3373	0.185		H = 30KG Series 2	
3.3413	3.4002	0.191			
3.4035	3.4689	0.198	1.1615	1.2246	0.118
3.4711	3.5339	0.206	1.2733	1.3415	0.094
3.5352	3.5956	0.215	1.3931	1.4631	0.092
3.5961	3.6541	0.223	1.5213	1.5946	0.087
3.6541	3.7098	0.233	1.6522	1.7387	0.089
3.7091	3.7794	0.241	1.7939	1.8949	0.092
3.7777	3.8442	0.256	1.9457	2.0425	0.097
3.8426	3.9068	0.265	2.0878	2.1805	0.104
3.9042	3.9671	0.270	2.2203	2.3060	0.110
3.9651	4.0241	0.289	2.3408	2.4540	0.118
4.0209	4.0785	0.296	2.4828	2.5879	0.126
4.0751	4.1447	0.310	2.6117	2.7115	0.132
			2.7315	2.8399	0.137
	H = 30KG Series 1		2.8558	2.9613	0.140
			2.9735	3.0758	0.144
1.2313	1.2967	0.099	3.0844	3.1827	0.149
1.3528	1.4207	0.095	3.1878	3.2815	0.156
1.4825	1.5708	0.087	3.2838	3.3731	0.164
1.6337	1.7203	0.089	3.3730	3.4577	0.173
1.7807	1.8659	0.091	3.4564	3.5368	0.182
1.9230	2.0045	0.096	3.5348	3.6113	0.192
2.0571	2.1487	0.102	3.6081	3.6921	0.200
2.1950	2.2814	0.109	3.6881	3.7683	0.209
2.3224	2.4043	0.116	3.7635	3.8394	0.222
2.4399	2.5307	0.123	3.8351	3.9072	0.234
2.5619	2.6487	0.129	3.9030	3.9719	0.245
2.6762	2.7593	0.134	3.9666	4.0509	0.252
2.7827	2.8638	0.137	4.0457	4.1441	0.266
2.8836	2.9625	0.141			
2.9794	3.0689	0.143		H = 40KG Series 1	
3.0824	3.1686	0.148			
3.1785	3.2607	0.155	1.1449	1.2169	0.128
3.2686	3.3472	0.162	1.2493	1.3300	0.099
3.3529	3.4271	0.172	1.3700	1.4376	0.122
3.4314	3.5038	0.176	1.4847	1.5675	0.096

Table I (cont.)

T(initial) °K	T(final) °K	C_H Joules/mole-°K
1.6150	1.6961	0.099
1.7464	1.8394	0.103
1.8887	1.9814	0.102
2.0281	2.1179	0.106
2.1621	2.2503	0.109
2.2894	2.3771	0.113
2.4115	2.4937	0.118
2.5235	2.6153	0.123
2.6404	2.7294	0.126
2.7509	2.8364	0.131
2.8534	2.9360	0.135

H = 40KG   Series 2

1.1514	1.2058	0.152
1.2474	1.3159	0.118
1.3618	1.4328	0.114
1.4829	1.5601	0.103
1.6139	1.6929	0.101
1.7464	1.8251	0.101
1.8786	1.9563	0.103
2.0086	2.0839	0.106
2.1347	2.2080	0.109
2.2576	2.3282	0.114
2.3755	2.4554	0.118
2.4984	2.5761	0.122
2.6148	2.6896	0.126
2.7236	2.7947	0.133
2.8227	2.8900	0.141

FIG. 7. 40 kG heat capacity for sample Pr III.

comparisons should be mentioned. First, is the fact that the magnitude of the heat capacity is again different, so that no two samples of "pure" Pr have

change between 2 and 4°K is 136 mJ/mole-°K at zero field and 95 mJ/mole-K° at 30 kG. There is then a 35% change in entropy upon the application of a 30,000 G magnetic field.

(3) It can be seen that the low-temperature upturn in the heat capacity occurs at higher temperatures as the magnetic field is increased. For example, the heat capacity at 1.4°K increases from 73.4 mJ/mole°K to 92.4 mJ/mole°K upon application of a 30,000 G field.

Upon completion of measurements on the sample designated Pr III, it was deemed necessary to investigate another praseodymium sample to determine if the above results could be reproduced. Sample Pr II was inserted into the apparatus and measurements were obtained after the application of a 30-kG field.

The first set of experimental data on sample Pr II is plotted in Fig. 8. The experimental observations are given in Table II.

Although the same general features apply to Sample Pr II as to Sample Pr III, some noteworthy
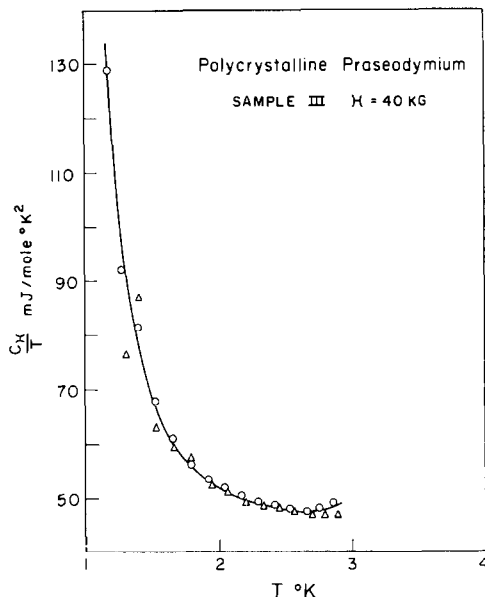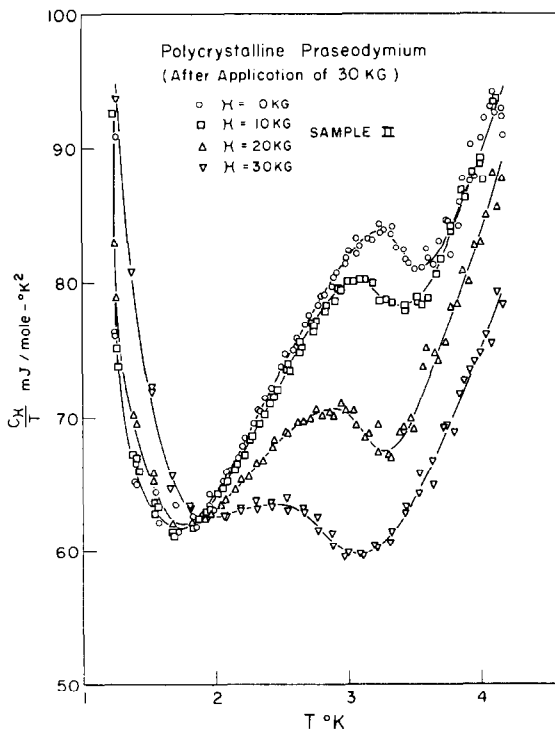

FIG. 8. In-Field heat capacity for sample Pr II (After application of a 30 kG field).

TABLE II

Experimental Heat Capacity Data for
Polycrystalline Praseodymium Sample Pr II

$T_{(initial)}$ °K	$T_{(final)}$ °K	C_H Joules/mole-°K	$T_{(initial)}$ °K	$T_{(final)}$ °K	C_H Joules/mole-°K
			2.5484	2.6163	0.194
			2.6383	2.7134	0.206
H = 0 Series 1			2.7323	2.8132	0.217
			2.8297	2.9174	0.229
1.2007	1.2946	0.095	2.9313	3.0144	0.242
1.3628	1.4592	0.092	3.0264	3.1050	0.255
1.5219	1.6136	0.097	3.1149	3.1912	0.262
1.6746	1.7602	0.106	3.1999	3.2831	0.271
1.8152	1.8947	0.115	3.2902	3.3706	0.280
1.9436	2.0234	0.125	3.3765	3.4568	0.279
2.0677	2.1487	0.139	3.4610	3.5398	0.283
2.1867	2.2595	0.152	3.5428	3.6270	0.296
2.2930	2.3608	0.164	3.6286	3.7123	0.296
2.3907	2.4545	0.175	3.7127	3.8000	0.318
2.4809	2.5519	0.186	3.7996	3.8835	0.330
2.5754	2.6421	0.198	3.8807	3.9614	0.343
2.6629	2.7366	0.210	3.9598	4.0444	0.363
2.7549	2.8359	0.221	4.0423	4.1232	0.380
2.8514	2.9297	0.232	4.1193	4.1991	0.384
2.9432	3.0168	0.244			
3.0283	3.0995	0.252			
3.1089	3.1854	0.263			
3.1939	3.2771	0.273	H = 0 Series 3		
3.2831	3.3652	0.278			
3.3703	3.4598	0.281	1.2251	1.2857	0.114
3.4639	3.5544	0.276	1.3470	1.4425	0.091
3.5566	3.6417	0.294	1.5040	1.5923	0.100
3.6420	3.7237	0.306	1.6483	1.7317	0.108
3.7233	3.8130	0.309	1.7842	1.8628	0.114
3.8115	3.9029	0.339	1.9124	1.9989	0.126
3.9015	3.9905	0.347	2.0431	2.1230	0.138
3.9869	4.0701	0.371	2.1631	2.2373	0.149
4.0668	4.1479	0.380	2.2732	2.3535	0.163
4.1424	4.2217	0.388	2.3857	2.4611	0.175
			2.4897	2.5598	0.189
H = 0 Series 2			2.5850	2.6519	0.198
			2.6749	2.7485	0.209
1.1967	1.2901	0.095	2.7686	2.8481	0.222
1.3582	1.4357	0.093	2.8656	2.9410	0.234
1.5023	1.5767	0.098	2.9569	3.0287	0.247
1.6406	1.7117	0.103	3.0421	3.1214	0.255
1.7708	1.8507	0.113	3.1333	3.2098	0.264
1.9031	1.9770	0.123	3.2200	3.3026	0.274
2.0238	2.0923	0.134	3.3114	3.4023	0.277
2.1338	2.2092	0.146	3.4086	3.4979	0.281
2.2453	2.3150	0.159	3.5041	3.5911	0.285
2.3471	2.4236	0.171	3.5944	3.6884	0.291
2.4518	2.5233	0.183	3.6910	3.7791	0.317

Table II (cont.)

T (initial) °K	T (final) °K	C H Joules / mole-°K		T (initial) °K	T (final) °K	C H Joules / mole-°K
3.7805	3.8760	0.322		3.8131	3.8964	0.335
3.8766	3.9640	0.354		3.8988	3.9842	0.347
3.9631	4.0493	0.358		3.9834	4.0672	0.353
4.0468	4.1272	0.385		4.0649	4.1454	0.384
4.1241	4.2053	0.378				

H = 10KG   Series 1

T (initial) °K	T (final) °K	C H Joules / mole-°K
1.1938	1.2620	0.114
1.3242	1.4209	0.092
1.4831	1.5754	0.098
1.6341	1.7220	0.103
1.7777	1.8589	0.112
1.9095	1.9977	0.123
2.0429	2.1237	0.136
2.1636	2.2510	0.148
2.2859	2.3666	0.162
2.3972	2.4726	0.174
2.4994	2.5704	0.186
2.5939	2.6716	0.197
2.6925	2.7659	0.209
2.7847	2.8646	0.220
2.8816	2.9574	0.232

H - 10KG   Series 2

T (initial) °K	T (final) °K	C H Joules / mole-°K
1.2296	1.3070	0.094
1.3753	1.4527	0.094
1.5193	1.5935	0.099
1.6589	1.7598	0.106
1.8181	1.9107	0.117
1.9631	2.0479	0.129
2.0946	2.1730	0.141
2.2143	2.3115	0.155
2.3476	2.4370	0.170
2.4683	2.5512	0.185
2.5785	2.6564	0.197
2.6807	2.7540	0.210
2.7755	2.8660	0.222
2.8847	2.9709	0.233
2.9872	3.0696	0.243
3.0835	3.1733	0.251
3.1851	3.2734	0.254
3.2839	3.3695	0.262
3.3782	3.4616	0.268
3.4688	3.5493	0.277
3.5550	3.6429	0.284
3.6468	3.7296	0.302
3.7327	3.8114	0.318

H = 10,000 Series 3

T (initial) °K	T (final) °K	C H Joules / mole-°K
1.2117	1.2889	0.094
1.3537	1.4312	0.094
1.4946	1.5703	0.096
1.6317	1.7037	0.102
1.7608	1.8277	0.111
1.8802	1.9555	0.121
2.0022	2.0719	0.132
2.1137	2.1786	0.143
2.2160	2.2881	0.154
2.3212	2.3887	0.166
2.4181	2.4816	0.177
2.5079	2.5679	0.188
2.5914	2.6687	0.199
2.6894	2.7628	0.210
2.7809	2.8506	0.221
2.8663	2.9338	0.228
2.9474	3.0313	0.239
3.0429	3.1239	0.247
3.1334	3.2326	0.255
3.2404	3.3598	0.260
3.3653	3.4811	0.267
3.4844	3.5954	0.278
3.5972	3.7236	0.295
3.7226	3.8404	0.317
3.8385	3.9496	0.336
3.9465	4.0517	0.355
4.0475	4.1451	0.384

H = 20,000   Series 1

T (initial) °K	T (final) °K	C H Joules / mole-°K
1.2240	1.2981	0.100
1.3606	1.4363	0.097
1.4976	1.5713	0.100
1.6320	1.7036	0.104
1.7603	1.8270	0.111
1.8793	1.9557	0.120
2.0028	2.0742	0.130
2.1166	2.1836	0.139
2.2216	2.2850	0.148
2.3192	2.3791	0.157
2.4102	2.4669	0.167
2.4947	2.5607	0.174

Table II (cont.)

T(initial) °K	T(final) °K	C_H Joules mole-°K	T(initial) °K	T(final) °K	C_H Joules mole-°K
2.5858	2.6579	0.182	4.1571	4.2389	0.419
2.6799	2.7492	0.190			
2.7689	2.8357	0.197	H = 30,000 G Series 1		
2.8531	2.9179	0.202			
2.9329	3.0054	0.209	1.4738	1.5577	0.109
3.0194	3.0906	0.212	1.6180	1.7012	0.109
3.1023	3.1722	0.216	1.7596	1.8393	0.114
3.1822	3.2513	0.217	1.8945	1.9703	0.121
3.2592	3.3387	0.222	2.0214	2.0929	0.129
3.3444	3.4286	0.233	2.1398	2.2204	0.138
3.4333	3.5140	0.243	2.2632	2.3390	0.147
3.5179	3.6020	0.263	2.3800	2.4524	0.154
3.6032	3.6939	0.273	2.4921	2.5729	0.162
3.6939	3.7816	0.282	2.6113	2.6895	0.168
3.7796	3.8715	0.300	2.7263	2.8020	0.173
3.8677	3.9653	0.314	2.8377	2.9240	0.174
3.9617	4.0538	0.333	2.9574	3.0405	0.180
4.0489	4.1341	0.361	3.0712	3.1514	0.186
4.1286	4.2123	0.366	3.1795	3.2560	0.194
			3.2817	3.3650	0.204
H = 20,000G Series 2			3.3881	3.4665	0.217
			3.4865	3.5702	0.232
1.1996	1.2856	0.103	3.5880	3.6701	0.236
1.3425	1.4329	0.097	3.6729	3.7487	0.257
1.4908	1.5783	0.101	3.7492	3.8330	0.262
1.6352	1.7200	0.105	3.8319	3.9098	0.282
1.7741	1.8536	0.113	3.9094	3.9932	0.293
1.9036	1.9780	0.122	3.9917	4.0809	0.307
2.0234	2.1061	0.132	4.0786	4.1716	0.327
2.1464	2.2234	0.143			
2.2594	2.3442	0.153	H = 30,000 G Series 2		
2.3755	2.4685	0.164			
2.4956	2.5836	0.175	1.2191	1.2833	0.117
2.6071	2.6903	0.184	1.3427	1.4099	0.111
2.7105	2.7896	0.194	1.4735	1.5558	0.109
2.8076	2.8842	0.200	1.6206	1.7038	0.108
2.8997	2.9731	0.209	1.7655	1.8445	0.114
2.9869	3.0709	0.213	1.9016	1.9765	0.122
3.0829	3.1657	0.214	2.0293	2.1001	0.129
3.1758	3.2636	0.224	2.1485	2.2278	0.138
3.2706	3.3584	0.223	2.2722	2.3476	0.146
3.3627	3.4456	0.236	2.3878	2.4596	0.154
3.4491	3.5401	0.242	2.4967	2.5781	0.160
3.5412	3.6331	0.270	2.6112	2.6890	0.168
3.6350	3.7256	0.273	2.7190	2.8072	0.170
3.7250	3.8187	0.295	2.8323	2.9172	0.177
3.8155	3.9041	0.312	2.9396	3.0234	0.178
3.9021	3.9959	0.327	3.0444	3.1367	0.185
3.9906	4.0801	0.343	3.1559	3.2439	0.194
4.0772	4.1638	0.353	3.2605	3.3567	0.201

Table II (cont.)

$T_{(initial)}$ °K	$T_{(final)}$ °K	C_H $\dfrac{Joules}{mole-°K}$
3.3702	3.4715	0.216
3.4815	3.5774	0.227
3.5864	3.6764	0.243
3.6832	3.7778	0.259
3.7833	3.8725	0.275
3.8748	3.9600	0.288
3.9621	4.0440	0.300
4.0415	4.1300	0.308
4.1250	4.2087	0.327

yet given the same value of the heat capacity in this temperature region. This can be seen in Fig. 9. Secondly, the kink has now become more distinct and appears as a Shottky-type anomaly which moves down in temperature as the field is increased. Thirdly, the low-temperature upturn occurs as a higher temperature than for Sample Pr III. Finally, the total heat capacity of Sample Pr II is higher than of Sample Pr III.

As a result of the remnant magnetization of Sample Pr II another series of in-field heat capacity measurements were taken in the following manner:

(1) The sample was heated and zero field magnetization data taken.

(2) The sample was warmed until no remnant magnetization was observed.

(3) The sample was cooled to He^4 temperatures in the absence of a magnetic field.

(4) No remnant magnetization was detected at 1.2°K.

(5) The heat capacity was determined as the applied field was increased from 0 to 30,000 G.

The heat capacity data obtained in Step 5 deviates from that given in Fig. 8 over all portions of the curve except at the 3.4°K kink. Note that the 30 kG curve of both runs superimpose. These results are shown in Fig. 10 and given in Table III.

Discussion of Results

1. The 3.4°K Anomaly

The nature of the 3.4°K kink in the heat capacity is not at all obvious. If, indeed, this is a property of pure praseodymium, the question arises as to the origin of the different values of the heat capacity for various samples.

One possibility is the formation of Pr^{4+}, the
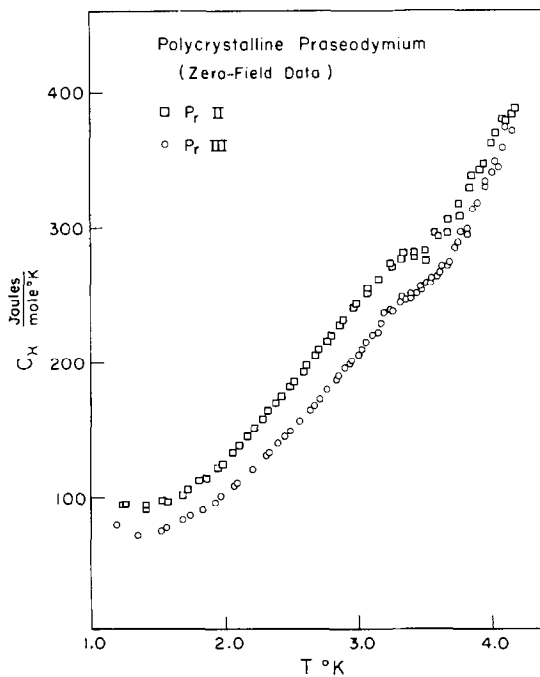
FIG. 9. A comparison of the heat capacity of samples Pr II and Pr III at zero-applied magnetic field.
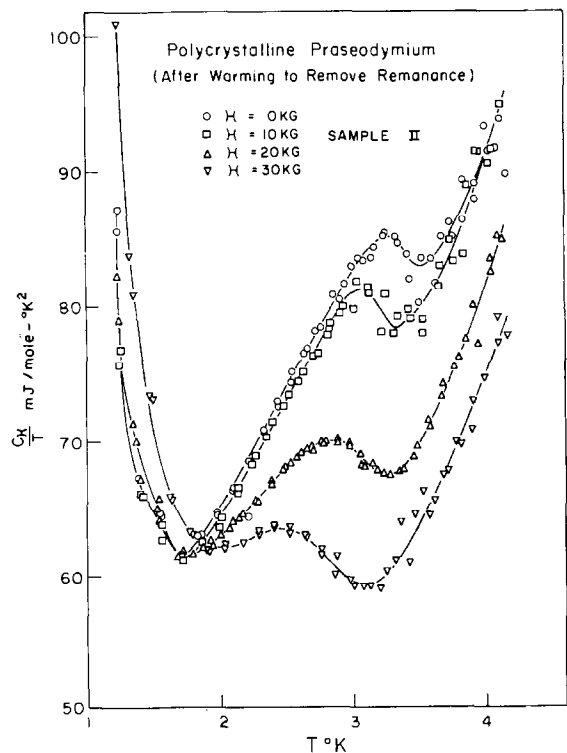
FIG. 10. In-Field heat capacity of sample Pr II after removal of remnant moment.

TABLE III

Experimental Heat Capacity Data for
Polycrystalline Praseodymium Sample II (after warming)

T(initial) °K	T(final) °K	C_H Joules/mole-°K	T(initial) °K	T(final) °K	C_H Joules/mole-°K
1.1870	1.2703	0.107	2.7109	2.7849	0.216
1.3346	1.4284	0.093	2.8129	2.8804	0.230
1.4932	1.5819	0.100	2.9067	2.9820	0.241
1.6439	1.7300	0.103	3.0065	3.0777	0.254
1.7843	1.8790	0.115	3.1006	3.1771	0.263
1.9265	2.0164	0.128	3.1987	3.2714	0.276
2.0579	2.1393	0.139	3.2910	3.3712	0.282
2.1757	2.2493	0.143	3.3895	3.4694	0.281
2.2816	2.3615	0.164	3.4866	3.5629	0.295
2.3897	2.4649	0.176	3.5810	3.6656	0.296
2.4900	2.5614	0.190	3.6827	3.7697	0.322
2.5839	2.6602	0.201	3.7850	3.8694	0.331
2.6793	2.7516	0.212	3.8836	3.9635	0.350
2.7684	2.8493	0.220	3.9762	4.0605	0.367
2.8621	2.9384	0.234	4.0655	4.1539	0.386
2.9513	3.0230	0.248	4.1550	4.2391	0.450
3.0331	3.1114	0.256			
3.1207	3.1959	0.266		H = 10,000 G Series 1	
3.2034	3.2757	0.277			
3.2810	3.3611	0.283	1.2024	1.2795	0.094
3.3660	3.4540	0.286	1.3517	1.4302	0.092
3.4558	3.5449	0.281	1.4999	1.5908	0.097
3.5440	3.6276	0.300	1.6589	1.7444	0.104
3.6273	3.7075	0.312	1.8059	1.8842	0.115
3.7062	3.7934	0.319	1.9397	2.0163	0.126
3.7888	3.8791	0.343	2.0660	2.1450	0.140
3.8759	3.9653	0.345	2.1898	2.2629	0.152
3.9589	4.0418	0.374	2.3045	2.3839	0.165
4.0354	4.1179	0.374	2.4222	2.4958	0.179
4.1092	4.1916	0.373	2.5316	2.6118	0.192
			2.6431	2.7310	0.205
	H = 0 Series 2		2.7588	2.8401	0.218
			2.8644	2.9415	0.231
1.1881	1.2731	0.105	2.9642	3.0479	0.240
1.3411	1.4354	0.093	3.0630	3.1473	0.252
1.5031	1.5923	0.100	3.1651	3.2447	0.251
1.6577	1.7429	0.105	3.2611	3.3482	0.258
1.8030	1.8811	0.116	3.3656	3.4577	0.272
1.9354	2.0076	0.127	3.4751	3.5660	0.275
2.0566	2.1234	0.139	3.5812	3.6755	0.296
2.1692	2.2432	0.151	3.6881	3.7761	0.317
2.2859	2.3544	0.165	3.7894	3.8759	0.321
2.3946	2.4583	0.177	3.8854	3.9717	0.359
2.4955	2.5666	0.188	3.9768	4.0616	0.364
2.6009	2.6797	0.203	4.0652	4.1526	0.390

Table III (cont.)

T(initial) °K	T(final) °K	C_H Joules mole-°K	T(initial) °K	T(final) °K	C_H Joules mole-°K
H = 10,000 G Series 2			H = 20,000 G Series 2		
1.2054	1.2863	0.096	1.2056	1.2807	0.098
1.3613	1.4420	0.092	1.3502	1.4283	0.094
1.5142	1.5906	0.099	1.4932	1.5683	0.098
1.6627	1.7350	0.105	1.6345	1.7067	0.103
1.8043	1.8826	0.116	1.7673	1.8405	0.111
1.9478	2.0198	0.128	1.8954	1.9641	0.120
2.0798	2.1581	0.141	2.0136	2.0802	0.130
2.2128	2.2967	0.156	2.1248	2.1945	0.140
2.3458	2.4229	0.171	2.2341	2.3023	0.149
2.4670	2.5391	0.184	2.3375	2.4019	0.158
2.5787	2.6464	0.196	2.4336	2.5117	0.168
2.6820	2.7561	0.208	2.5395	2.6136	0.177
2.7877	2.8572	0.222	2.6382	2.7154	0.186
2.8861	2.9615	0.234	2.7371	2.8155	0.194
2.9892	3.0604	0.248	2.8342	2.9098	0.201
3.0880	3.1673	0.253	2.9263	2.9998	0.206
3.1935	3.2700	0.261	3.0138	3.0864	0.208
3.2958	3.3710	0.264	3.0985	3.1791	0.214
3.3947	3.4770	0.272	3.1888	3.2784	0.219
3.4993	3.5884	0.280	3.2873	3.3965	0.227
3.6081	3.6907	0.303	3.4029	3.5066	0.238
3.7098	3.7987	0.313	3.5106	3.6077	0.255
3.8142	3.8956	0.343	3.6105	3.7226	0.272
3.9095	3.9868	0.361	3.7249	3.8527	0.289
3.9928	4.0764	0.369	3.8533	3.9714	0.313
			3.9726	4.0826	0.337
H = 20,000 G Series 1			4.0828	4.1143	0.349
1.1966	1.2689	0.101	H = 20,000 G Series 3		
1.3413	1.4166	0.097			
1.4876	1.5612	0.099	1.2975	1.4058	0.097
1.6310	1.7362	0.104	1.4764	1.5812	0.100
1.7981	1.8934	0.115	1.6485	1.7843	0.106
1.9485	2.0357	0.126	1.8448	1.9674	0.120
2.0842	2.1728	0.137	2.0227	2.1343	0.133
2.2152	2.2974	0.148	2.1858	2.2880	0.147
2.3347	2.4117	0.159	2.3354	2.4299	0.160
2.4445	2.5223	0.169	2.4731	2.5611	0.172
2.5513	2.6251	0.179	2.6004	2.6832	0.183
2.6508	2.7272	0.186	2.7189	2.7975	0.193
2.7500	2.8228	0.195	2.8300	2.9055	0.201
2.8428	2.9129	0.203	2.9345	3.0076	0.207
2.9309	2.9992	0.208	3.0345	3.1065	0.209
3.0148	3.0850	0.211	3.1303	3.2104	0.215

Table III (cont.)

T(initial) °K	T(final) °K	C_H Joules/mole-°K	T(initial) °K	T(final) °K	C_H Joules/mole-°K
3.2319	3.3096	0.221	1.8709	1.9471	0.119
3.3281	3.4136	0.229	1.9962	2.0822	0.127
3.4293	3.5102	0.242	2.1260	2.2073	0.135
3.5232	3.6101	0.254	2.2465	2.3230	0.145
3.6207	3.7028	0.269	2.3600	2.4450	0.153
3.7106	3.7976	0.284	2.4795	2.5605	0.161
3.8040	3.8942	0.306	2.5938	2.6844	0.166
3.8997	3.9878	0.313	2.7163	2.8045	0.170
3.9904	4.0821	0.333	2.8347	2.9194	0.177
4.0818	4.1690	0.351	2.9488	3.0449	0.178
			3.0738	3.1659	0.185

H = 30,000 G   Series 1

T(initial) °K	T(final) °K	C_H Joules/mole-°K	T(initial) °K	T(final) °K	C_H Joules/mole-°K
1.1582	1.2283	0.148	3.1946	3.2817	0.196
1.2839	1.3647	0.111	3.3079	3.3878	0.214
1.4269	1.5097	0.108	3.4162	3.5028	0.223
1.5740	1.6577	0.106	3.5249	3.6195	0.230
1.7202	1.8026	0.112	3.6375	3.7255	0.248
1.8610	1.9384	0.118	3.7422	3.8345	0.265
1.9927	2.0791	0.126	3.8467	3.9354	0.276
2.1280	2.2092	0.135	3.9453	4.0370	0.298
2.2541	2.3306	0.145	4.0420	4.1381	0.316
2.3722	2.4445	0.154			
2.4848	2.5546	0.159			
2.5942	2.6727	0.166			
2.7113	2.7876	0.171			
2.8253	2.9006	0.172			
2.9362	3.0088	0.178			
3.0420	3.1244	0.183			
3.1546	3.2452	0.189			
3.2715	3.3561	0.203			
3.3791	3.4609	0.209			
3.4814	3.5551	0.233			
3.5733	3.6546	0.238			
3.6711	3.7577	0.252			
3.7686	3.8508	0.266			
3.8610	3.9471	0.285			
3.9547	4.0367	0.299			
4.0446	4.1208	0.323			
4.1269	4.2025	0.325			

H = 30,000 G   Series 2

T(initial) °K	T(final) °K	C_H Joules/mole-°K
1.1884	1.2576	0.133
1.3135	1.3953	0.109
1.4548	1.5366	0.109
1.5963	1.6793	0.108
1.7375	1.8175	0.112

amount of Pr^{4+} formed being different for each sample. This would give rise to the apparent differences in the heat capacity of each sample and would be dependent upon the sample history, i.e., whether it was annealed, vacuum distilled and then remelted, not retreated, etc. If Pr^{4+} were truly forming at these low temperatures, then the 3.4°K anomaly could be attributed to the chemical formation of these ions; the low-temperature upturn to the magnetic ordering of Pr^{4+}. Ce, praseodymium's neighbor in the rare-earth series, does show some evidence of Ce^{4+} formation. Ce^{3+}, which has one $4f$ electron, will give up its electron to deplete the $4f$ level, finding it energetically favorable to do so. Pr, on the other hand, upon forming Pr^{4+} would still have one $4f$ electron, and the formation of Pr^{4+} would not lower the total energy of the system. It is thus highly doubtful that Pr^{4+} ions exist in praseodymium metal.

Another possibility is that the samples studied were not truly polycrystalline. This seems unreasonable, however, because of the large size of all the samples (at least 100 g) involved. In addition, when Sample Pr II was rotated 90°, the magnetization results were not altered. If any preferred orientation were present, the magnetization would be expected to vary with the orientation of the sample.

Let us now consider the effect of impurities. Such an effect would lead to different heat capacity results for each sample tested. If we consider impurities are present in the praseodymium, then there is in effect, a dilute alloy of the impurity atom in a Pr matrix. Praseodymium has a structure with the ABAC stacking sequence so that there exists in the Pr lattice two separate sites, a cubic site, and a hexagonal closed packed site (20), each giving rise to its own crystalline field. The antiferromagnetic state at 25°K found by Cable et al. (6) exists on one site, most likely the hexagonal, while the cubic sites remain unordered. If this be the case, then magnetic impurities may scatter the Pr conduction electrons and give rise to a resistance minima or Kondo effect (21). Such an effect was found by Nagasawa and Sugawara (22) on measurements of dilute Pr–Ce and La–Pr alloys. Although their praseodymium sample showed no magneto-resistive minima, the resistance did flatten out below 4°K. With the addition of as little as 0.5 at. % Ce, a resistance minima was found.

Schreiffer (23) has suggested that in this temperature region, the localized magnetic moment of the impurity may be totally compensated by the conduction electrons which have been polarized at the impurity site. This effect is thought of as one in which the wavefunction of each Pr electron is perturbed, the net effect being that this perturbation leads to an effective condensation of condition electrons at the impurity site in an antiferromagnetic mode.

If this Kondo condensation takes place as described above, then at some temperature there must be a phase transition associated with this compensated antiferromagnetic state, but the effect on the entropy would be quite small. Our in-field heat capacity measurements indicate that the 3.4°K anomaly is indeed small and shows a definite movement to lower temperatures as the field is increased, as expected for an antiferromagnetic phase transition.

Unfortunately, if one accepts this viewpoint, there are several questions which are left unanswered. One is the fact that the magnetization versus temperature curve (see Fig. 2) does not show any evidence of a transition occurring near 3.4°K in either sample. Sensitivity of the instrumentation would allow an observation of moment changes corresponding to the small amount of entropy involved in this transition. Another is the remnant moment which is observed on Sample Pr II but not Sample Pr III. That no zero-field moment was established on Sample Pr III may mean that the impurity content was so low that no moment could be detected or that the type of impurity present allowed for a complete Kondo condensation. The remnant moment on Pr II would indicate an uncompensated impurity by the Kondo mechanism, although this situation seems unlikely.

Probably the most damaging argument is the fact that nonmagnetic cubic site (which is necessary for Kondo condensation) will not explain the low-temperature upturn results (vide infra).

Impurities may still be the answer to the problem. If oxides were forming, these might give rise to the observed behavior. One can only speculate here also, as there is no experimental data on praseodymium oxides that we know of in this temperature region.

It is of further interest to note that although the temperature at which the 3.4°K peaks occur is different for both samples, the critical field versus critical temperature curves parallel each other for the two samples studied (see Fig. 11). This indicates that the mechanism involved in the antiferromagnetic coupling is the same.

2. The Low-Temperature Upturn

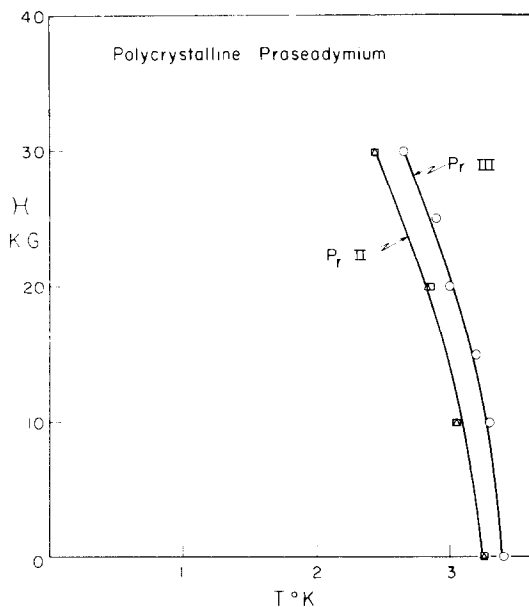The low-temperature upturn is also problematic. On Sample Pr III, the low-temperature upturn

FIG. 11. Loci of heat capacity maxima for samples Pr II and Pr III as a function of temperature and applied magnetic field.

substantially moves up in temperature with an applied field of only 10,000 G.

In an attempt to obtain a rough estimate of the nuclear field, the zero-field heat capacity upturn of Sample Pr II was fit to the equation

$$C_N = R\left[\frac{Q''}{Q} - \left(\frac{Q'}{Q}\right)^2\right] \qquad (1)$$

where

$$Q = \sum_i e^{-\epsilon_i/kT}, \qquad (2)$$

$$Q' = \sum_i \frac{\epsilon_i}{kT} \epsilon^{-\epsilon_i/kT}, \qquad (3)$$

$$Q' = \sum_i \left(\frac{\epsilon_i}{kT}\right)^2 \epsilon^{-\epsilon_i/kT}, \qquad (4)$$

where i is the energy eigenvalue of the i-th state and is given by

$$i = \mu_N \gamma_N H_N \cdot I_n, \qquad (5)$$

where I_n is Pr nuclear moment; H_N is nuclear field; γ_N is the nuclear gyromagnetic factor; μ_N is the nuclear Bohr magneton.

Fitting the zero-field upturn to Eq. (1) gives a nuclear field of the order of 5.83×10^5 G. Applying a perturbation of 30-kG external magnetic field has little effect on this hyperfine interaction. Yet in both samples there is a significant effect in the experimental results.

A comparison of the in-field heat capacity curves of the two Pr samples reveals that the heat capacity of Sample Pr II is not field dependent up to 20 kG while that of Sample Pr III is highly field dependent.

Bleaney (3) has noted that to explain the anomalously large heat capacity upturn (assuming singlet ground states) of praseodymium, terms are needed to account for an exchange mechanism strong enough to give rise to a ferromagnetic interaction in the metal. Lounasmaa (14) has suggested that ferromagnetic clusters from on the fcc sites giving rise to the large observed low-temperature heat capacity. The present data show that in both praseodymium samples the upturn in the heat capacity increases in temperature with applied field, suggesting that the onset of ferromagnetic ordering is occurring.

The ferromagnetic coupling appears to be more enhanced in Sample Pr II than in Sample Pr III. The different behavior of the two samples must be connected in some way to the remnant moment of Sample Pr II. The impurity present in the sample (as evidenced by the remnance) enhances the onset of magnetic ordering the resultant behavior of the low-temperature upturn. The mechanism for this ordering is unknown.

Crystal field calculations indicate a singlet ground state on the fcc sites. However, the M vs T curve (see Fig. 2) indicate a constantly increasing value of magnetization as the temperature is decreased. A singlet ground state and resultant Van Vleck Paramagnetism would not account for this result. A constantly increasing moment together with the infield heat capacity measurements indicate the onset of long-range order with ferromagnetic coupling.

Acknowledgments

References

1. D. A. PARKINSON, F. E. SIMON, AND R. H. SPEDDING, Proc. Roy. Soc. Ser. A 207, 137 (1951).
2. B. BLEANEY, Proc. Roy. Soc. Ser. A 276, 39 (1963).
3. B. BLEANEY, J. Appl. Phys. 34, 1022 (1963).
4. J. M. LOCK, Proc. Roy. Soc. Ser. B 70, 566 (1957).
5. P. GRAF, Z. Angew. Phys. 13, 534 (1961).

6. J. W. CABLE, R. M. MOON, W. C. KOEHLER, AND E. O. WOLLAN, *Phys. Rev. Lett.* **12**, 553 (1964).

7. D. A. PARKINSON, F. E. SIMON, AND F. H. SPEDDING, *Proc. Roy. Soc. Ser. A* **207**, 137 (1951).

8. W. E. WALLACE AND R. S. CRAIG, Proposal to Army Research Office, Durham, 1967.

9. O. V. LOUNASMAA AND L. J. SUNDSTROM, *Phys. Rev.* **158**, 591 (1967).

10. F. N. KISSELL, Ph.D. Thesis, University of Pittsburgh, 1965.

11. W. E. WALLACE, F. N. KISSELL, E. SEGAL, AND R. S. CRAIG, *J. Phys. Chem. Solids* **30**, 13 (1969).

12. B. DREYFUS, B. B. GOODMAN, A. LACAZE, AND G. TROLLIET, *C.R. Acad. Sci.* **253**, 1764 (1961).

13. C. W. DEMPSEY, J. E. GORDON, AND T. SOLLER, *Bull. Amer. Phys. Soc.* **7**, 309 (1962).

14. O. V. LOUNASMAA, *Phys. Rev.* **133**, 211 (1964).

15. M. DIXON, unpublished results.

16. Research Chem., Division of Nuclear Corp, Phoenix, Arizona.

17. Performed by Mr. J. Johnson, Westinghouse Electric, Pittsburgh, Pa.

18. Performed by Dr. E. Hodge, Mellon Institute, Pittsburgh, Pa.

19. O. V. LOUNASMAA, *Phys. Rev.* **133**, 211 (1964).

20. K. A. GSCHNEIDER, "Rare Earth Alloys," D. van Nostrand Co. Inc., New Jersey, 1961.

21. J. KONDO, *Progr. Theor. Phys.* **32**, 37 (1964).

22. H. NAGASAWA AND T. SUGAWARA, *J. Phys. Soc. Jap.* **23**, 701 (1967).

23. J. R. SCHREIFFER, *J. Appl. Phys.* **38**, 1143 (1967).